

A Theoretical Fluid Dynamic Model for Estimation of the Hold-up and Liquid Velocity in an External Loop Airlift Bioreactor

Konstantina Koutita^a

Alessandro M. Lizzul^b

Luiza C. Campos^a

Nithin Rai^c

Tristan W. P. Smith^d

Julia A. Stegemann^a

^aCentre for Resource Efficiency & the Environment
Department of Civil
Environmental and Geomatic Engineering
University College London
Gower Street, London
United Kingdom
WC1E 6BT

^bCentre for Urban Sustainability and Resilience
University College London
Gower Street, London, United
Kingdom, WC1E 6BT

^cOctoply Ltd.
34 Armstrong Road
Royal Arsenal, London
United Kingdom
SE18 6RS

^dEnergy Institute
University College London
14 Central House, Upper Woburn Place
London, United Kingdom
WC1H 0HY

Abstract

This article demonstrates a new simplified mathematical model developed for an external loop airlift bioreactor, derived from recognised chemical engineering formulae, with the minimum possible reliance on empirical correlations with adjustable parameters. Bubble slip velocity, liquid circulation velocity and gas hold-up are simply estimated based on bubble diameter, gas flow rate, riser diameter and riser height. The model reveals the contribution of bubble diameter to gas hold-up and liquid circulation velocity, filling a gap in the literature. Bubble size is known as an important variable for optimising gas absorption and energy input. Validation of the model is conducted using our own and other experimental data. The current model was found to provide a better estimate of gas hold-up than the literature model compared with, but liquid velocity was overestimated. The impact of using various drag coefficient correlations was also revealed.

Keywords: airlift bioreactors, fluid dynamic model, gas hold-up, liquid velocity, algae

Introduction

Airlift bioreactors encompass a broad family of pneumatic gas-liquid contacting devices, in which gas injected into the reactor “riser” causes circulation of liquid via a linked “downcomer” due to a density difference. The circulatory patterns are a function of the geometry and velocity within the system and differ from the flow in a bubble column (Shah, Kelkar, Godbole, *et al.*, 1982). Airlift bioreactors have a wide range of applications in bio processing, chemical processing and wastewater treatment (Merchuk & Siegel 1988; Moo-Young & Chisti 1994); in particular, they have a variety of operational benefits for cultivation of algae, including high gas and mass transfer, increased exposure to light due to uniform turbulent mixing, low hydrodynamic stress and ease of control, particularly of liquid velocity (Kumar, Dasgupta, Nayak, *et al.*, 2011). They also display flatter dissolved oxygen profiles compared to bubble columns (Chisti, 1989), with the circulation velocity and oxygen removal characteristics reported to be closely linked (Molina, Fernández, Acién, *et al.*, 2001).

The objective of our work was to develop and validate a simple macroscopic fluid dynamic model for an external loop airlift bioreactor at steady state, to estimate how the bubble slip velocity, liquid circulation velocity and gas hold-up are influenced by the bubble diameter, gas flow rate and reactor geometry. This novel model was derived from recognised chemical engineering formulae, with the minimal possible reliance upon empirical correlations. The model is validated against existing and new experimental data and compared to the well-known model by Chisti (1989), which incorporates an empirical correlation to estimate gas hold-up; it has been widely validated for a great range of sizes and configurations of algal airlift reactors, which need longer circulation loops for photosynthesis than airlift reactors used for other biological or chemical processes (Fernandez, Sevilla, Perez, *et al.*, 2001).

Modelling Requirements

Figure 1 illustrates common airlift reactor configurations, with either an internal or external loop. Bubble size within airlift reactors is usually of 0.5–5 mm (Shah *et al.* 1982; Zimmerman *et al.* 2011), but can expand in the upper portion of longer tubes.

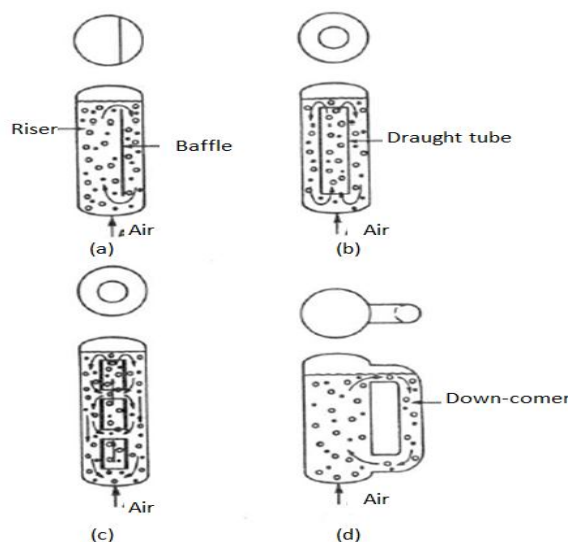


Figure 1: Types of Airlift Bioreactors: (A) Split-Cylinder Internal-Loop; (B) Concentric Draught-Tube Internal-Loop; (C) Draught-Tube Internal-Loop with Vertically Split Draught-Tube; (D) External Loop (Chisti, 1989)

Bitog *et al.* (2011), Merchuk (2003) and Petersen and Margaritis (2001) have reviewed airlift fluid dynamic models. Discrepancies in literature relationships between gas hold-up, superficial gas velocity, effect of any solid phase and column diameters were found to be due to different measuring techniques. Review of two- and three-phase system models by Merchuk (2003) showed discrepancies in model predictions to be due to use of different drag coefficients and frictional loss estimates, as well as the fact that many models are configuration specific. They emphasised the lack of a generalised equation with wide range validity and requirements for massive data to validate the empirical correlations proposed by some studies. Bitog *et al.* (2011) showed the progress in computational fluid dynamics studies, mostly of bubble columns employing the Eulerian-Eulerian mixture model.

They confirmed the lack of a systematic method for scale-up and highlighted the importance of drag coefficient estimation for algal systems.

Only a few studies have examined the effect of bubble size, gas flow rate and reactor dimensions on flow characteristics: Law & Battaglia (2013) and Zhang et al. (2005) examined gas hold-up and liquid velocity dependence for bubbles with the same average size but different distributions; Camarasa et al. (2001) studied the effect of bubble size on the gas hold-up and the pressure but the range of bubble diameters was small (2–2.5 mm); Saez et al. (1998) introduced the buoyancy force in the model by Young et al. (1991) for computationally intensive modelling of the effect of bubble size on the gas hold-up and the liquid velocity, but validated it for only one size; Marquez et al. (1999) further introduced a differential equation to estimate the phase change due to reaction in this model but their experimental results are restricted to one gas flow rate.

The existing studies for external loop reactors are based on two parallel approaches, either using continuity and momentum balance equations (Camarasa et al. 2001; Young et al. 1991), or power balance equations (Chisti 1989; García-Calvo et al. 1999). Our proposed model is macroscopic and uses a mean bubble size within the reactor, which allows the momentum balance to be omitted and only an overall mechanical power balance to be used instead. This work resolves some of the literature deficiencies by using a simple generalised equation, validating the model for several reactor sizes and bubble sizes, and by examining whether existing drag coefficient correlations can sufficiently describe the behaviour of the examined bubble size range. Results for the estimation of liquid circulation velocity support the design of airlift reactors, i.e. liquid circulation velocity determines allowable riser tube length, depending on the gas flow rate and riser diameter.

Modelling Approaches

Power Balance Approach

Our approach uses equilibrium of forces applied on the bubbles to estimate their relative velocity. The model then uses the power conservation principle on the gas/liquid mixture in the bioreactor to estimate the liquid circulation velocity and the gas hold-up in the riser. As shown in

Figure 2, the buoyancy force acting upon individual bubbles is opposed by the counteracting drag force from the water. As the bubbles enter the bioreactor, they reach their equilibrium slip velocity in very short time, implying that the buoyancy force is balanced by the drag. When considering a small fraction of the mixture (bubbles with liquid); the power provided by the buoyancy force is balanced by the power consumed by the frictional forces of the walls and the connections.

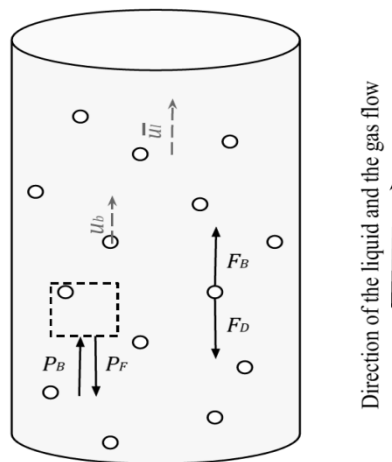


Figure 2. Section of the riser tube. The relative velocities of the bubbles and the liquid are shown, alongside the forces acting on each according to the power balance approach. u_b is the bubble slip velocity, u_l the liquid circulation velocity, F_B and P_B the force and power from buoyancy, F_D the drag force and P_F the power from friction.

The buoyancy force acting on a bubble and the interfacial drag force imposed by the surrounding liquid upon each bubble are described respectively by the following equations (Kuiper, 2010):

$$F_B = (\rho_l - \rho_g) g \frac{\pi d_b^3}{6} \quad (1)$$

$$F_D = \frac{1}{2} c_D \rho_l u_b^2 \pi \frac{d_b^2}{4} \quad (2)$$

where F_B is the buoyancy force, ρ_l and ρ_g are the liquid and gas densities, respectively, d_b is the bubble diameter, F_D is the drag force, u_b is the bubble slip velocity, and c_D is the drag coefficient calculated from Ishii and Zuber (1979) formula for the particles in the viscous flow regime:

$$c_D = \frac{24}{Re_b} (1 + 0.1 Re_b^{0.75}) \text{ for } Re_b < 2 \cdot 10^5 \quad (3)$$

$$\text{where } Re_b = \frac{u_b d_b}{\nu_l} \quad (4)$$

where ν_l is the kinematic viscosity of the liquid. This drag coefficient correlation is a classical one used extensively in the literature, including for similar experiments (Sáez, Marquez, Roberts, *et al.*, 1998); the impact on the model of using other common formulae (Karamanev & Nikolov 1992; McCabe *et al.* 1956; Morisson 2013; Sáez *et al.* 1998) for the drag coefficient is discussed in section 5.4. Buoyancy and drag forces are applied to the total riser height. The number of bubbles is calculated using the following expression:

$$N = \frac{V_g}{\frac{1}{6} \pi d_b^3} = \frac{q_g}{\frac{1}{6} \pi d_b^3 t_g} = \frac{q_g}{\frac{1}{6} \pi d_b^3 u_b + \bar{u}_l} l_r \quad (5)$$

where N is the number of bubbles, V_g is the volume of the gas, q_g is the gas flow rate, t_g is the gas residence time in the riser, l_r is the riser height (i.e. vertical length) and \bar{u}_l is the liquid circulation velocity.

Considering the force components along the longitudinal axis of the riser, the buoyancy forces should be equal to the sum of the drag forces for the total riser height (Chisti, 1989).

$$\sum F_{B_x} = \sum F_{D_x} \Rightarrow N (\rho_l - \rho_g) g \frac{\pi d_b^3}{6} = N \frac{1}{2} c_D \rho_l u_b^2 \pi \frac{d_b^2}{4} \quad (6)$$

Using the formulae in Eqs. 3, 4 and 6, the expression for the bubble slip velocity is:

$$u_b = \sqrt{\frac{4 g d_b (\rho_l - \rho_g)}{3 \rho_l c_D}} \quad (7)$$

The residence times of the gas and the liquid, the gas hold-up in the riser, and the density of the mixture, are calculated from the following formulae, respectively:

$$t_g = \frac{l_r}{u_b + \bar{u}_l} = \frac{V_g}{q_g} \quad (8)$$

$$t_l = \frac{l_r}{\bar{u}_l} = \frac{V_l}{q_l} \quad (9)$$

$$\varepsilon_r = \frac{V_g}{V_{riser}} = \frac{l_r q_g}{\frac{\pi d_r^2}{4} l_r} = \frac{4 q_g}{\pi d_r^2 (u_b + \bar{u}_l)} \quad (10)$$

$$\rho_m = \frac{\rho_l q_l + \rho_g q_g}{q_l + q_g} \xrightarrow{\text{steady state}} \frac{\rho_l V_l + \rho_g V_g}{V_l + V_g} = \frac{\rho_l \left(\frac{\pi d_r^2}{4} - \frac{q_g}{\bar{u}_l + u_b} \right) + \rho_g \frac{q_g}{\bar{u}_l + u_b}}{\frac{\pi d_r^2}{4}} \quad (11)$$

where t_r is the residence time of the liquid during recirculation in the riser, V_l is the volume of the liquid in the reactor, q_l is the liquid flow rate, ε_r is the gas hold-up in the riser, V_{riser} is the riser volume, d_r is the riser diameter and ρ_m is the mixture density.

Additionally, the gas rise velocity and the superficial gas velocity are respectively estimated from the following formulae:

$$\bar{u}_g = \bar{u}_l + u_b \quad (12)$$

$$u_g = \bar{u}_g \varepsilon_r \quad (13)$$

where \bar{u}_g is the gas rise velocity and u_g the superficial gas velocity.

Considering the force components along the longitudinal axis in

Figure 2 under steady conditions, the supplied buoyancy power must overcome the wall friction of the mobilised fluid (with upward circulation velocity). Therefore, the power provided by the buoyancy force in the riser tube must be equal to the power consumed by the friction loss along the reactor. This balance of powers defines the steady flow velocity of the liquid-gas mixture. The two balancing powers are given as:

$$P_B = (\rho_l - \rho_g) g \frac{\pi d_b^3}{6} Nu_b \quad (14)$$

$$P_F = \Delta p \cdot q_l = \rho_l g q_l h \quad (15)$$

where P_B is the power provided by buoyancy, P_F is the power lost to friction, Δp is the pressure difference and h is the head due to friction, given as:

$$h = h_f + h_m = f \frac{l \bar{u}_l^2}{d_r 2g} + K_l \frac{\bar{u}_l^2}{2g} \quad (16)$$

where h_f and h_m are the head losses due to wall friction and fitting friction, respectively. K_l is the additional frictional loss coefficient, and $f = \frac{64}{Re}$ for Reynolds number of the liquid $Re_l < 2100$. For $Re_l \geq 2100$, f is calculated from the Churchill formula (Anon, 1999):

$$f = \left\{ -4 \log \left[0.27 \frac{r}{d_r} + \left(\frac{7}{Re_l} \right)^{0.9} \right] \right\}^2 \quad (17)$$

With the Reynolds number found by the Blasius equation (for $Re < 80,000$) (Anon, 1999):

$$Re_l = \frac{v_l d_r}{\nu_l} \quad (18)$$

The term coupled with K_l in Eq. 16 is the sum of the frictional losses expressed as the frictional velocity head losses due to expansions, K_{exp} , contractions, K_{contr} and fittings, K_{fit} in the loop.

By equating the power input with the output, the model is simplified to represent the liquid velocity and can be solved by iteration, for given parameters of the fluid characteristics, including reactor diameter, riser and reactor length (which is the sum of the riser and down comer heights plus the connection lengths), bubble diameter and gas flow rate, and after first solving Eq. 7:

$$\bar{u}_l^3 (\bar{u}_l + u_b) = \frac{\delta g (\rho_l - \rho_g) u_b q_g l_r}{\pi d_r \rho_l \left[K_l d_r + l \left\{ -4 \log \left[0.27 \frac{r}{d_r} + \left(\frac{7 \bar{u}_l}{\nu_l d_r} \right)^{0.9} \right] \right\}^2 \right]} \quad (19)$$

The following assumptions were made in developing our model:

For the estimation of the bubble slip velocity from Eq. 7, an average bubble size along the tube was used. This does not mean that the isothermal gas expansion of the bubble along its propagation is not considered, as the use of the buoyancy force in the equations implies that density is different at different reactor heights.

Bubbles are considered spherical; bubbles have been reported to be spherical for a $d_b < 1$ mm and ellipsoid for $1 \text{ mm} < d_b < 1 \text{ cm}$ (Clift, Grace & Weber, 1978).

The Reynolds number of the bubbles' slip in the liquid is always below the threshold required by Eq.3, based on estimates of $Re_b = 170 - 2,200$ in the experiments.

Bubbles have negligible weight compared to the drag and buoyancy forces.

The gas flow rate is constant.

Flow is at steady state.

Flow is turbulent.

The drag force is uniform over the cross-section of the tube as bubbles are assumed to be spread evenly after a short distance from their entrance into the bioreactor.

There is negligible bubble recirculation (Chisti, 1989).

Bubbles wake friction is negligible.

The gas is assumed to instantly obtain the temperature of the liquid by the time it is sparged into it, so compression due to temperature difference of the two phases is not accounted.

Chisti's Airlift Bioreactor Model

For an external-loop airlift, where the top and bottom connections are very similar in geometry, Chisti (1989) estimates the superficial liquid velocity as:

$$u_l = \sqrt{\frac{2gh_D(\varepsilon_r - \varepsilon_d)}{k_B \left(\frac{1}{(1-\varepsilon_r)^2} + \left(\frac{a_r}{a_d}\right)^2 \frac{1}{(1-\varepsilon_d)^2} \right)}} \quad (20)$$

where u_l is the superficial liquid velocity, h_D is the dispersion height, ε_d is the gas hold-up in the downcomer, k_B is the frictional loss coefficient for the bottom connecting section of the reactor tubes, a_r and a_d are the cross-sectional areas of the riser and downcomer, respectively. The values for ε_r and ε_d are estimated from the following empirical formulae:

$$\varepsilon_r = \frac{u_g}{0.24 + 1.35(u_g + u_l)^{0.93}} \quad (21)$$

$$\varepsilon_d = 0.79\varepsilon_r - 0.057 \quad (22)$$

The frictional loss coefficient for the connecting section in the present study is assumed to have a mean value of $k_B = 5$ (Chisti, 1989) and the gas hold-up in the down comer is assumed negligible.

Computational Algorithms and Parameters

Figure 3 illustrates the interrelation of the parameters in the two approaches and

Figure 4 shows the computational algorithm referring to the equations used to estimate the liquid circulation velocity in each of the two approaches. The models were solved using MathWorks MATLAB Version 7.11.0.584 (R2010b). The whole simulation ran in less than a minute with MATLAB 7.11.0 (R2010b) on a 32-bit Intel(R) Core(TM) i5 CPU.

Although the two approaches follow the same path, there is a difference in the energy inputs and outputs used. The energy input from the bubble inflow is expressed in our model as the power from the buoyancy force, whereas in Chisti's model it is the isothermal gas expansion. The energy outputs considered in our power balance approach are due to the wall and fitting friction loss and the drag force, whereas Chisti's model considers the energy dissipation due to wakes behind the bubbles, energy loss due to stagnant gas and to fluid turn-around friction. Secondly, in its present form, our model is for riser and down comer tubes of identical diameters and would need modification to describe other systems. Finally, Chisti's model uses empirical formulae for riser and down comer gas hold-up, which may be configuration dependent (e.g. ε_r in Eq. 22 has to be higher than 0.07 in order to give a rational positive ε_d figure, so ε_d was assumed to be zero in Eq. 20 and 22 for our calculations).

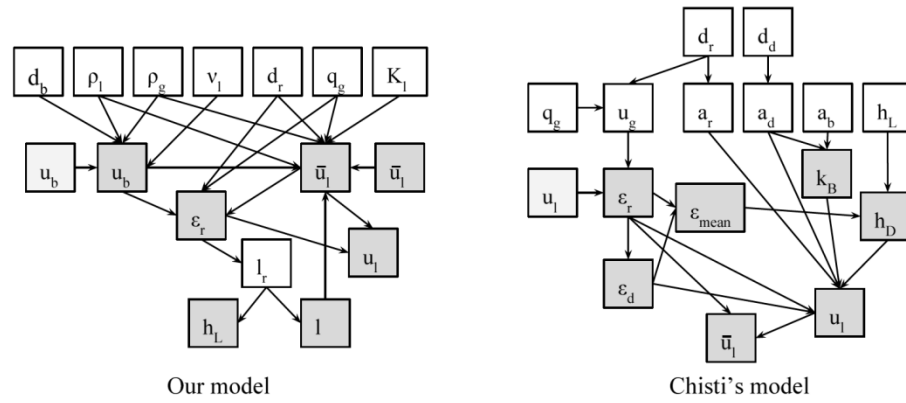


Figure 3. The interrelations between parameters within the two models. Left: the power balance approach developed in the present work, Right: the model developed by Chisti (1989). White boxes: given parameters, light grey boxes: assumed values, dark grey boxes: estimated.

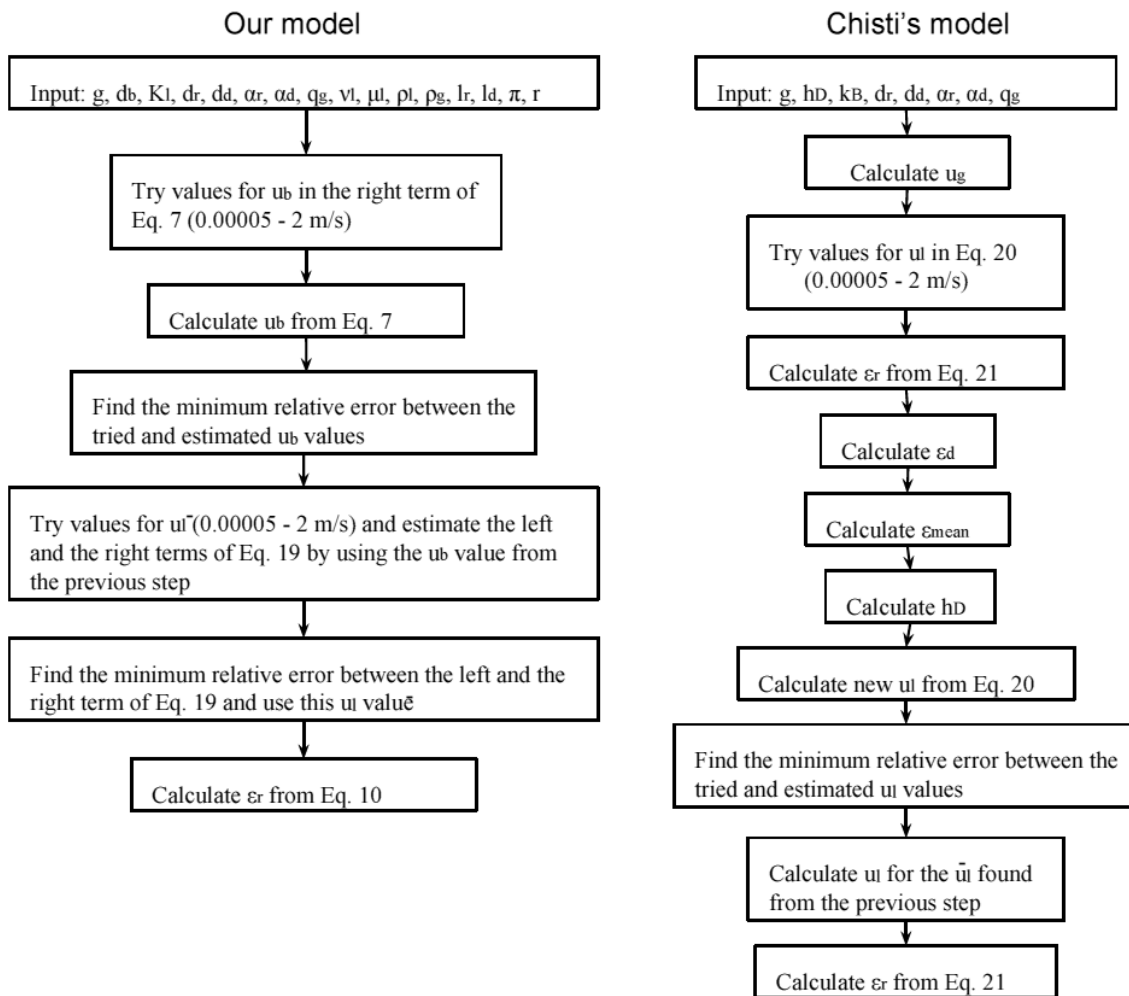


Figure 4: Computational Algorithms for the Estimation of the Liquid Circulation Velocity and Gas Hold-Up in the Riser from the Two Different Models

Experimental Determination of the Gas Hold-Up and Liquid Circulation Velocity– Statistical Analysis Methodology

Experimental Reactor

The experimental reactors were constructed from standard polyvinyl chloride piping connectors and polymethyl methacrylate tubing for riser and down comer sections (Plastock). Five different reactor configurations were used which differed in diameter and height in order to examine their influence on the results. The dimensions of reactors R1, R2, R3, R4 and R5 are shown in

Table 1 and are based on designs from the unpublished work of Lizzul. Information for estimation of the frictional losses is shown in

Table 2. The expansions and contractions are located at the points where flow passes from the main pipes to the fittings and from the fittings to the main pipes, respectively. The 180° close return bends are located at the top of the reactors where liquid passes from the riser to the down comer, whereas the 90° standard and square L fittings are at the bottom of the down comer and riser, respectively. Each reactor was filled with tap water to the middle of the horizontal degasser zone as shown in Figure 5.

The gas was fed by an air-compressor (Hailea AC0-009E 112W), of maximum output 140 L/min and pressure output >0.035 MPa. The ambient temperature during the experiments was 23°C and the temperature of the water was 16°C. Three spargers of different porosities were used to conduct experiments with three different average bubble sizes. The first two spargers were 3D-printed from nylon beads. Sparger D1 was slightly perforated and D3 was more perforated. The third sparger (sparger D2) was a porous ceramic sparger.

Table 1: Dimensions of the Reactors

Reactors	d_r (m)	d_d (m)	l_r (m)	l_d (m)	l (m)	h_d (m)
R1	0.054	0.054	1.04	1.04	2.40	1.04
R2	0.054	0.054	2.04	2.04	4.40	2.04
R3	0.058	0.058	0.54	0.54	1.40	0.54
R4	0.10	0.10	1.04	1.04	2.40	1.04
R5	0.034	0.034	1.04	1.04	2.40	1.04

Table 2: Estimation of the Frictional Losses (Velocity Head Loss)

Loss types	K_l Estimation	Values (Anon, 1999)	Frequency in reactors				
			R1	R2	R3	R4	R5
K_{fit}	180° close returns bends	1.5	2	2	2	2	2
	90° standard L	1.3	1	1	1	1	1
	90° square L	0.75	1	1	1	1	1
K_{contr}	$\sum_{i=1}^n 0.5 \left(1 - \frac{a_{i+1}}{a_i}\right)$	0.4177	2	4	2	2	2
K_{exp}	$\sum_{i=1}^n \left(1 - \frac{a_i}{a_{i+1}}\right)^2$	0.2464	2	4	2	2	2

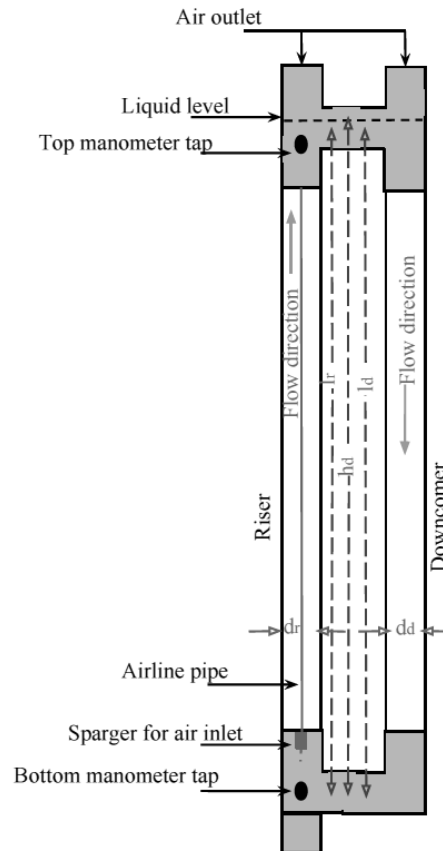


Figure 5: Schematic of the External Loop Reactors Used for the Experiments (Dimensions are Shown in Table 1)

Bubble Size Measurement

The effects of bubble size on gas hold-up and liquid velocity were examined experimentally using flights of bubbles produced from the three different spargers with different steady-state gas flow rates. The flights of bubbles were photographed with a high ISO setting on a Nikon D40x lens, 18-55mm. For each photograph, areas of up to 25 bubbles were measured using the open access software ImageJv 1.47 (NIH) (Softonic International S.L., 2014) and used to calculate average equivalent bubble diameters (the term equivalent will be omitted henceforth for simplicity). This sample size gave an approximate 28% precision with a measured mean variance 0.2 mm and for 95% confidence level, according to the sample size estimation by Reck how and Chapra(1983). The probabilities, p , that the shown effects of repeat measurements are attributable to random error, were determined based on a one-way analysis of variance (ANOVA). An effect is generally considered as statistically significant when $p < 0.05$. The p values between the different bubbles measured for the two runs were 0.19 and 0.74; therefore, only one measurement from each condition was used for the calculations in this paper.

To determine whether the size of the bubbles changed as a function of the height of the reactor, bubbles were measured at the bottom, middle and top of the riser, at 0.1 m, 0.5 m and 0.9 m, respectively, for the three spargers in reactor R1. Bubbles were then measured at the heights 0.1 m, 0.9 m and 1.9 m, for the three spargers in another reactor with double height, but with the same diameter and geometry (reactor R2). In both reactors, sparger D1 showed monotonically increasing bubble diameter with increasing gas flow rate and height (Figure 6).

Sparger D2 also shows an increase in bubble diameter with increasing gas flow rate and riser height, but with a shallower slope. However, for sparger D3 there was a slight decrease in bubble diameter with increasing height, which could be due to bubbles splitting during their rise in high turbulence. The performance of the three spargers shows that, in both reactors, sparger D1 gives the lowest bubble diameter output followed by sparger D2 and sparger D3. The mean bubble sizes and average standard deviations for the sparger measurements in the two set-ups (R1 and R2) are shown in (table 3).

The results of a three-way ANOVA were approximated by the use of a regression equation with three factors in Excel. The probabilities p that the effect of the sparger and the gas flow rate on the bubble size is attributable to random error were $2.1 \cdot 10^{-15}$ and 0.015 for reactor R1, respectively, and $5.3 \cdot 10^{-6}$ and 0.16 for reactor R2. However, the effect of the height in the reactor is statistically insignificant as the probability was 0.961 and 0.334 for reactors R1 and R2, respectively. To simplify calculations, the variation of the bubble diameter as a function of the gas flow rate was not taken into account in the validation of the model, and bubble diameters of 2.2, 3.3, 4.6mm (average values between the two reactors from table 3 were used in the model).

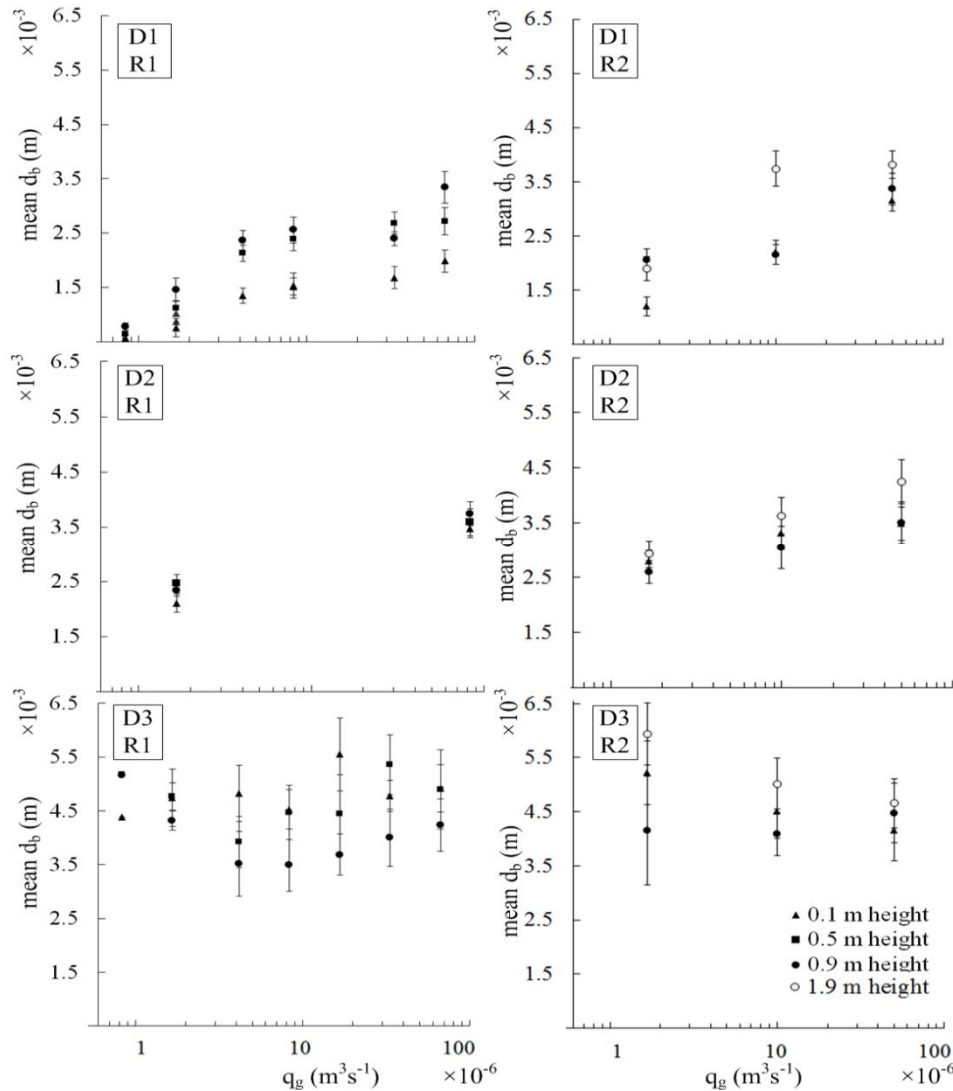


Figure 6. Bubble diameter measured at different heights of the riser as a function of gas flow rate for the three spargers (D1, D2 and D3) in the reactor configurations R1 (left) and R2 (right) along with the 95% confidence intervals (CI) calculated from the standard deviation and the sample mean.

Table 3: Bubble Diameters for Different Spargers

Sparger	Measurements for reactor R1		Measurements for reactor R2	
	Mean bubble diameter (mm)	Standard deviation (mm)	Mean bubble diameter (mm)	Standard deviation (mm)
D1	1.8	0.5	2.6	0.7
D2	3.3	0.5	3.3	0.7
D3	4.4	0.6	4.7	1.0

Gas Hold-Up and Liquid Velocity Measurement

Gas hold-up was measured using a U-bend manometer as suggested by Molina et al. (2001). Liquid circulation velocity was measured following the bubble measurements using a tracer injection of 0.8 mM acetic acid, detected by a pH probe (Jenway). The water was refreshed after each measurement of velocity. The recirculation time was determined as the average duration between 3 peaks and between three troughs of the pH. The liquid circulation velocity was calculated by dividing the length of the reactor loop by the average recirculation time. One to three replicates were undertaken for each experimental condition to examine the repeatability of the method. The average standard errors among the average velocities for different gas flow rates were 0.0176 ms^{-1} , 0.0095 ms^{-1} and 0.0091 ms^{-1} for spargers D1, D2 and D3, respectively. ANOVA indicated that the probabilities p that the effect of the sparger or the gas flow rate on the liquid velocity are attributable to random error were greater than 0.95.

Results and Discussion

Basic Model Validation for Gas Hold-Up Results

Figure 7 to 9 show measurements of the gas hold-up in the riser as a function of the gas flow rate, compared with predictions for the two modelling approaches.

Figure 7 examines the influence of bubble diameter. Results from our model, using the parameter values from Table 1 and

Table 2, are presented as different solid lines for the three bubble diameters (spargers) in reactor R1, while results from Chisti's model, which is independent of d_b , are shown with a dashed line. Results for riser gas hold-up from Chisti's model are closest to the results from our model for $d_b = 3.3 \text{ mm}$, which suggests that bubbles of this size might have been used for the development of the empirical Eq. 21 in Chisti's model. Our model shows that gas hold-up in the riser decreases with increasing bubble diameter, as drag coefficient and bubble slip velocity increase and thus less gas is retained in the reactor at a particular time. However, this is not validated by the experimental data. The dependence of the measured gas hold-up on bubble diameter appears minor in this figure.

Figure 8 shows the influence of riser diameter with $d_b = 4.6 \text{ mm}$ in our model and experiments. The selected limits used for the riser diameter are typical of the literature. The influence of the riser height is shown in Figure 9, again with $d_b = 4.6 \text{ mm}$ in our model and experiments. Similar behaviour and figures (not shown) were obtained for the other two spargers. The two models give similar gas hold-up results for all gas flow rates. In all cases the models overestimate the gas hold-up, relative to the experiments, with an average relative error between our model and our experimental data of 59%, whereas the average relative error between Chisti's model and our experimental data is 93%.

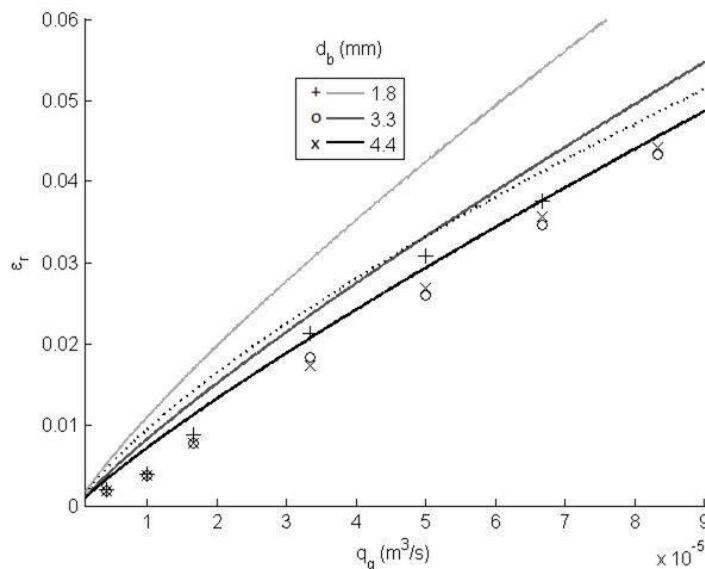


Figure 7: Measurements of gas hold-up as a function of the gas flow rate in reactor R1 for the bubble diameters indicated, compared with predictions from our model (solid lines) for various diameters and Chisti’s model (dotted line)

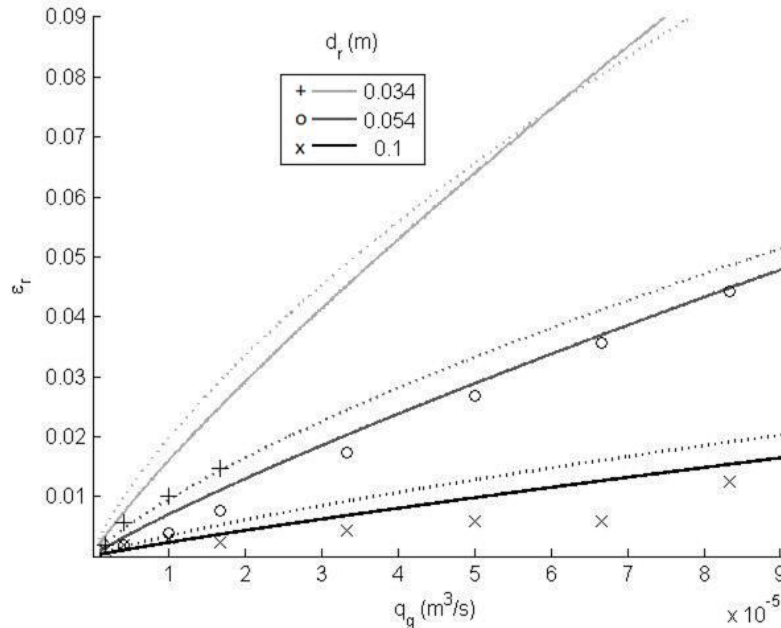


Figure 8: Measurements of gas hold-up as a function of gas flow rate in reactors R1, R4 and R5, for the three different riser diameters indicated and using sparger D3, compared with predictions from our model (solid lines) and Chisti’s model (dotted lines).

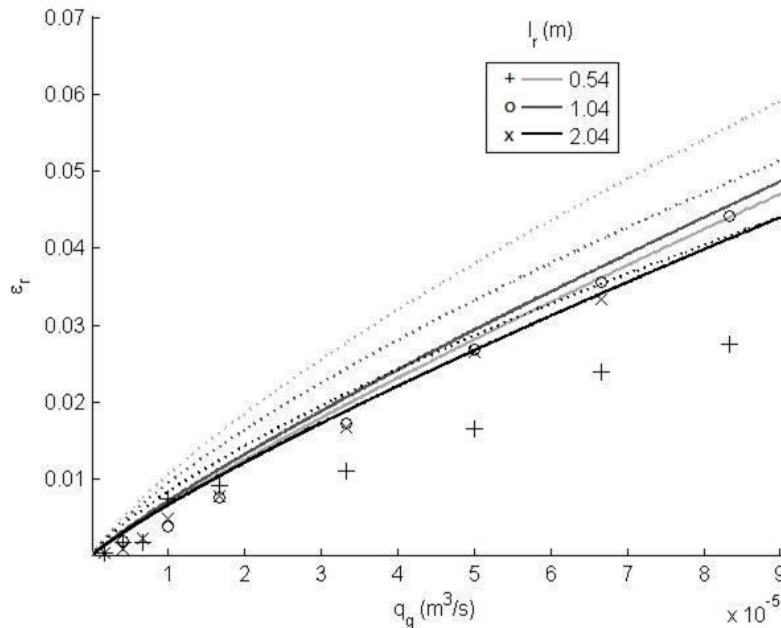


Figure 9: Measurements of gas hold-up as a function of the gas flow rate in reactors R1, R2 and R3, for the three different riser heights indicated and using sparger D3, compared with predictions from our model (solid lines) and Chisti’s model (dotted lines).

Basic Model Validation for Liquid Circulation Velocity Results

The results for the bubbles slip velocity predicted by our model are in agreement with Chisti’s(Chisti, 1989), and the assertion by Molina et al. (2001) that bubble slip velocities tend to range from 0.2 – 0.4 ms⁻¹.

Figure 10 to 12 show measurements of liquid circulation velocity as a function of the gas flow rate, examining the influence of bubble diameter, riser diameter and riser length, respectively. Both modelling approaches predict that the liquid circulation velocity increases with gas flow rate, which accords with experiment results.

The average relative error between our model and our set of experimental data for the liquid velocity is 31%, whereas the average relative error between Chisti's model and our experimental data is 11%.

Moreover, the models were also compared to experimental data for various bubble diameters of two studies from the literature (Camarasa et al. 2001; Marquez et al. 1999) in

Figure 13 to Figure 15. The fit to our model is better apart from the liquid velocity data in Figure 15, but there is a lack of literature measurements of liquid velocities for different bubble sizes to verify this observation.

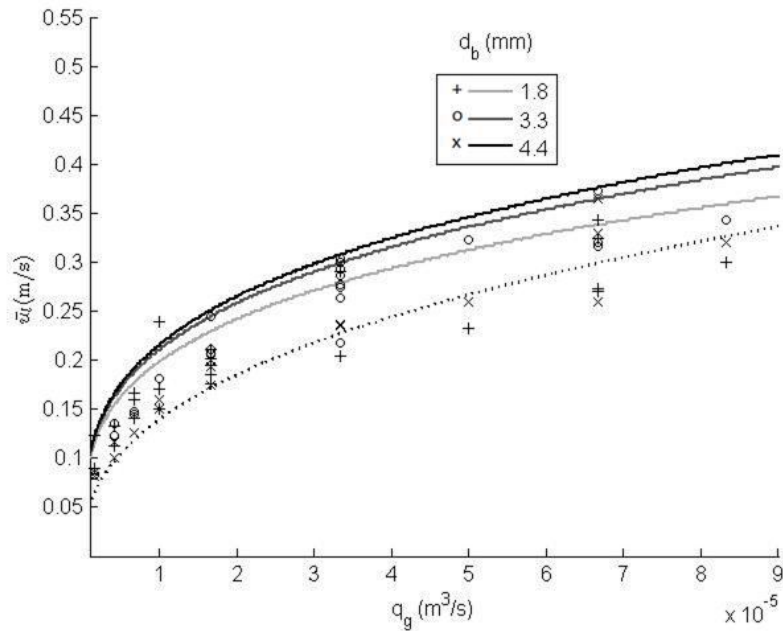


Figure 10: Measurements of liquid circulation velocity as a function of the gas flow rate in reactor R1 for the three bubble diameters indicated, compared with predictions from our model (solid lines) for various bubble diameters and Chisti's model (dotted line)

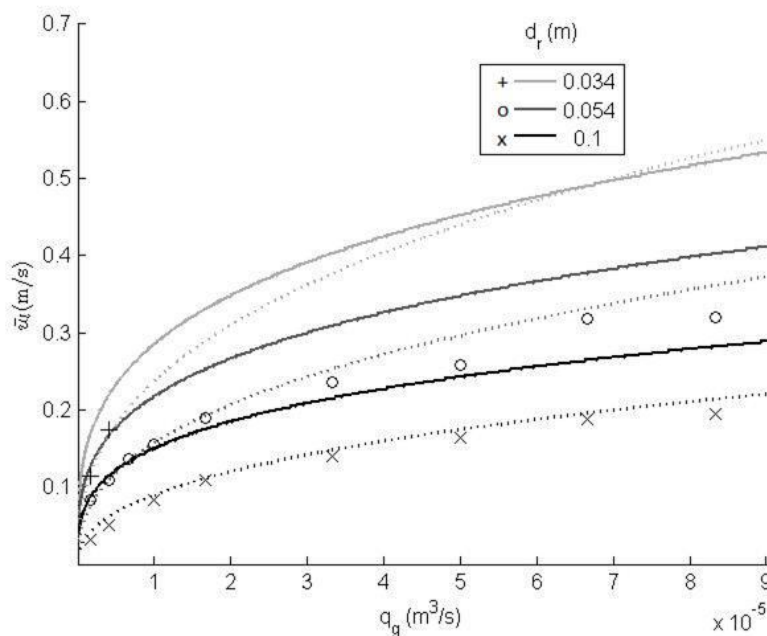


Figure 11: Measurements of liquid circulation velocity as a function of the gas flow rate in reactors R1, R4 and R5, for the three different riser diameters indicated and using sparger D3, compared with predictions from our model (solid lines) and Chisti's model (dotted lines)

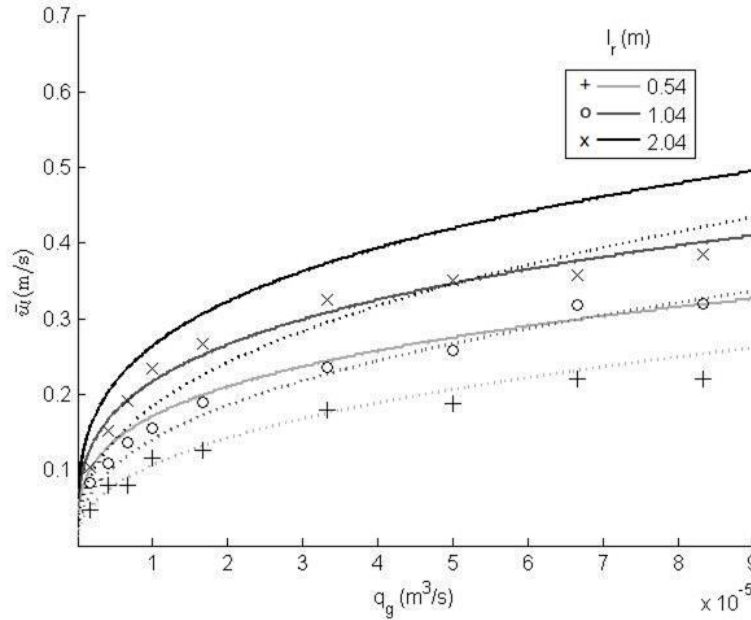


Figure 12: Measurements of liquid circulation velocity as a function of the gas flow rate in reactors R1, R2 and R3, for the three different riser heights indicated and using sparger D3, compared with predictions from our model (solid lines) and Chisti's model (dotted lines)

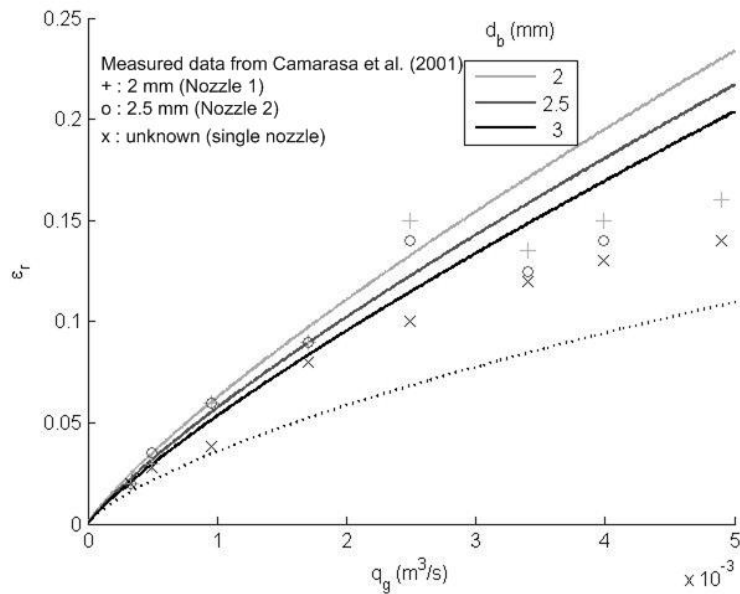


Figure 13: Measurements of gas hold-up by Camarasa et al. (2001) in an airlift reactor with a riser diameter of 0.23 m and riser length of 3.50 m as a function of the gas flow rate, compared to predictions from our model (solid lines) for various diameters and Chisti's model (dotted line).

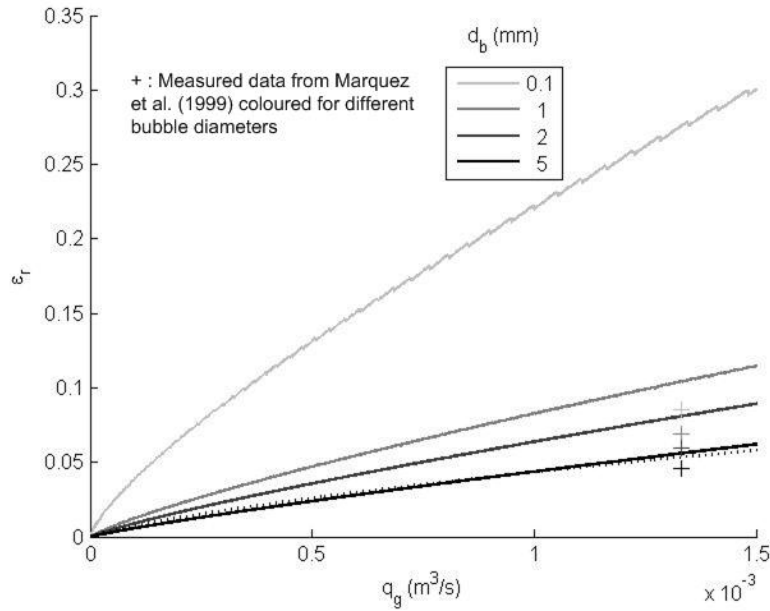


Figure 14: Measurements of gas hold-up by Marquez et al. (1999) in an airlift reactor with a riser diameter of 0.19 m and riser length of 1.56 m as a function of gas flow rate, compared to predictions from our model (solid lines) for various diameters and Chisti’s model (dotted line).

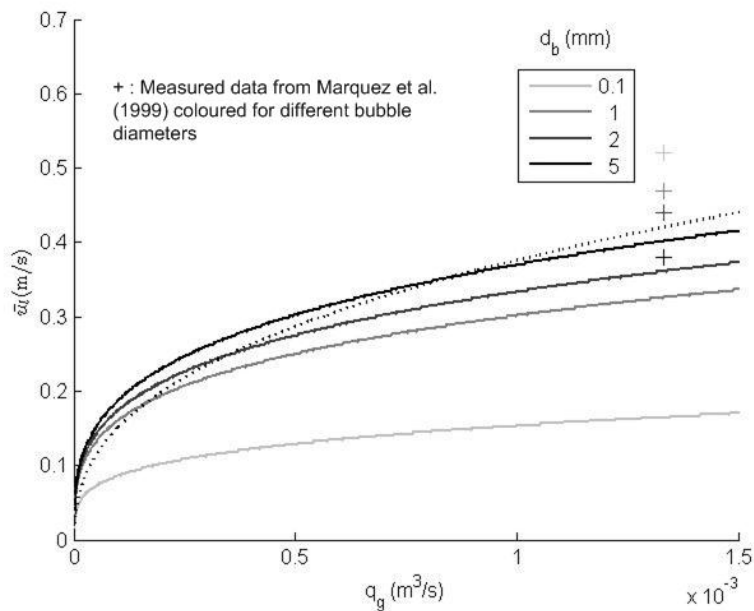


Figure 15: Measurements of liquid circulation velocity by Marquez et al. (1999) in an airlift reactor with a riser diameter of 0.19 m and riser length of 1.56 m as a function of gas flow rate, compared to predictions from our model (solid lines) for various diameters and Chisti’s model (dotted line).

Model Uncertainty and Experimental Errors

Uncertainties associated with our model include the assumptions of negligible bubble recirculation, spherical bubbles, and negligible friction of bubble wakes. There may be significant interfacial forces that are not considered. Overall, our model takes into account the integration of the main forces applied within the system and does not consider the micro-scale forces. Compared to Chisti’s model, it uses fewer algorithm steps, achieving results comparable to our own and other experiments, it is based on a simple consideration of explicit hydrodynamic factors and involves the minimal possible reliance on empirical equations that could limit the range of the model applicability. The fact that the measurements and the model give comparable results indicates that the major part of the involved physics has been adequately accounted for.

Differences between model predictions and experimental results could be caused by either model or experimental inadequacies. Gas hold-up is overestimated by both models compared to our experiments, which may be caused by our assumption of a single bubble diameter, whereas bubble size distribution has been shown to affect both the average gas hold-up and the distribution of gas within the reactor (Law & Battaglia, 2013). Also, the possible change in volumetric gas flow rate due to the temperature difference between the heated compressed gas and the bubbles after cooling by the water has not been taken into account.

Our experimental results for the liquid velocity are likewise overestimated by our model, which may be attributable to the energy loss from turbulence produced by the bubbles and to small quantities of stagnant gas observed in the down comer, especially at higher gas flows. Also, the surface tension developed upon addition of the acetic acid may have influenced the liquid velocity experiments. On the other hand, Chisti's model appears to underestimate liquid circulation velocity at lower gas flow rates, as his model incorporates more friction forces.

Figure 7 and 10 show that the sensitivity of the gas hold-up and the liquid circulation velocity to the bubble diameter is lower than expected. A clear order of the liquid circulation velocity output from the different spargers used is difficult to distinguish in Figure 10 due to the sensitivity of the repeat measurements to factors such as the purity of the water and the gas flow meter adjustments. In addition, the influence of the drag coefficient on the liquid velocity is discussed below (5.4). The impression that the bubble size does not contribute as significantly as the gas flow rate to the liquid velocity could be further investigated using a targeted series of experiments, e.g., with a wider range of bubble sizes.

Effect of Different Drag Coefficient Correlations

The differences between our model and experimental data were greater when other drag coefficients for spherical shapes were used. For example, the correlations given by McCabe et al. (1956) (used by Chisti, 1989), Khan and Richardson (Sáez, Marquez, Roberts, *et al.*, 1998), Karamanev and Nikolov (1992) and Morisson (2013) gave errors in the gas hold-up of 72%, 66%, 150% and 67%, respectively; and in the liquid circulation velocity of 36%, 30%, 27% and 30%, respectively. As suggested by Sáez et al. (1998), these findings suggest that using an improved drag coefficient correlation could model fit. However, the use of different existing correlations did not lead to significant convergence of the models' curves, or give outputs that matched the order of the experimental data in

Figure 7. Bubbles with 1-10 mm diameter are ellipsoidal, lacking symmetry and oscillating in shape. Also, especially for air bubbles in water, their slip velocity is sensitive to the presence of surfactants (Clift, Grace & Weber, 1978). Curves given by Gaudin(1957) for distilled water and water with surfactants do not converge for ellipsoidal bubbles where surface tension forces are important(Clift et al. 1978; Gaudin 1957).

There is a need to determine a correlation for bubbles of size range where their shape and flow regime changes from spherical to ellipsoid shapes. Various published results for air bubbles in water do not show good agreement, mostly due to differences in water purity, wall effects and measurement techniques (Clift et al. 1978;Gaudin 1957; McCabe et al. 1956). When data for correlation of bubble size to bubble rise velocity from experiments by Baker and Chao in McCabe et al. (1956), Taylor in Gaudin's work (1957), and Clift et al. (1978) were used in our model, gas hold-up estimation errors were found to be 95%, 100% and 100%, respectively; and liquid circulation velocity estimation errors were 28%, 28% and 28%, respectively. Apart from the small differences in errors, the data gave different orders in the curves for the different bubble diameters and only Baker and Chao's data gave the same order found in our experiments in (figure 7). Therefore, the development of an appropriate new drag coefficient correlation for bubbles in the examined flow regime may substantially improve fluid dynamic models for airlift reactors. Also, well defined bubble shapes and optimally spherical bubbles would not only follow the current model better but would also give higher liquid circulation velocities, though this may be hard to influence.

Conclusions

This paper presents a novel approach for the estimation of the liquid circulation velocity. The model developed was validated by comparison both with our own and other experimental results, and with the results from Chisti's well-known semi-empirical model(1989).Our model has a purely theoretical basis, allowing calculation of liquid velocity without the need for empirical expression for the gas hold-up. Thus, our model is useful for estimation of gas hold-up and liquid velocity, and calculating optimal airlift reactor geometry, in applications where the conditions deviate from assumptions associated with the empirical formulae. Importantly, this model differs from Chisti's in that it shows the potential impact that the bubble diameter can have on gas hold-up and liquid velocity.

Predictions for gas hold-up and liquid circulation velocity from our model were comparable to experimental results over a range of values of gas flow rate, riser diameter, riser height, and bubble diameter, though the effect of varying the bubble diameter could not always be distinguished experimentally. Different drag coefficient correlations clearly affected model predictions and errors relative to the experimental data; improvement of the drag coefficient estimation is therefore recommended for good model fit.

Acknowledgements

We would like to express our thanks for the support of UCL Impact Award, EPSRC and industrial sponsors Octoply and Varicon Aqua Solutions, without which this project would not have been possible. We also extend our gratitude to the Royal Commission for the Exhibition of 1851 for providing financial support towards A. M. Lizzul's project. Finally, we would like to thank H. Arevalo-Bacon and R. Beckett of the Bartlett for their assistance with the design and manufacturing of the novel sparger types, as well as A. Lekuona for his assistance with some of the liquid velocity measurements, and A. Chow for his help with statistical analysis.

Notation

Roman Characters

- a_j : Cross-sectional area of the down-comer (m^2)
- a_i : Cross-sectional area of a fitting with different diameter from the main tube (m^2)
- a_r : Cross-sectional area of the riser (m^2)
- c_D : Drag coefficient (dimensionless)
 - : Mean diameter of the bubbles (mm)
 - : Diameter of the downcomer tube (m)
 - : Diameter of the riser tube (m)
 - : Buoyancy force (N, or kgms^{-2})
 - : Drag force (N, or kgms^{-2})
 - : Darcy-Weisbach friction factor (dimensionless)
 - : Gravitational acceleration (ms^{-2}). The value of 9.810 was used for this fixed parameter as a modelling input.
- h : Head due to friction (m)
 - h : Height of the liquid in the riser after gas entrance, hence height of the dispersion (m)
 - h : Head due to sum of friction on the wall (m)
 - h : Height of the liquid in the riser before gas entrance (m)
 - : Head due to friction in the fittings (m)
 - : Frictional loss coefficient for the bottom connecting section of the reactor tubes (dimensionless). The value of 5.0 was used for this fixed parameter as a modelling input.
 - : Equivalent frictional velocity head loss due to contractions (dimensionless)
 - : Equivalent frictional velocity head loss due to expansions (dimensionless)
 - : Equivalent frictional velocity head loss from the fittings in the loop (dimensionless)
 - : Additional frictional loss coefficient, equivalent number of frictional velocity head loss
- : Total length of the bioreactor (m)
 - : Length of the down-comer (m)
 - : Length of the riser (m)
- : Number of bubbles in the tube (dimensionless)
 - : Power generated from the buoyancy force (W)
 - : Power consumed by the friction on the wall and the fittings (W)
- : Pressure (Pa or $\text{kgm}^{-1}\text{s}^{-2}$)
 - : Gas sparging rate (m^3s^{-1}). Values within the range 0 – 0.0001 were used for this experimental input variable.
 - : Mean flow rate of the liquid (m^3s^{-1})
- : Relative roughness of the pipe (m). The value of 0.0000025 was used for this fixed parameter as a modelling input.
 - : Reynolds number (dimensionless)
 - : Reynolds number of the bubbles (dimensionless)
 - : Reynolds number of the mixture (dimensionless)
 - : Residence time of the bubbles in the riser (s)

- : Residence time of the liquid in the riser (s)
- : Mean velocity of bubbles in the riser relative to the liquid (ms^{-1})
- : Superficial gas velocity in the riser (ms^{-1})
- : Superficial liquid velocity of the liquid mobilised by the bubbles in the riser (ms^{-1})
- : Gas rise velocity in the riser estimated according to the sum of and (ms^{-1})
- : Liquid circulation velocity in the riser (ms^{-1})
- : Volume of gas in the riser tube (m^3)
- : Volume of liquid in the riser tube (m^3)
- : Volume of the riser (m^3)

Greek Characters

- : Gas hold-up in the down-comer (dimensionless)
- : Gas hold-up in the riser (dimensionless)
- : Mean gas hold-up in the reactor (dimensionless)
- : Dynamic viscosity ($\text{kgm}^{-1}\text{s}^{-1}$). The value of 0.798×10^{-3} was used for the fixed parameter of the liquid in the reactor as a modelling input.
- : Kinematic viscosity of water (m^2s^{-1}). The value of 0.801×10^{-6} was used for the fixed parameter of the liquid in the reactor as a modelling input.
- : Ratio of circumference to diameter of a circle (dimensionless). The value of 3.142 was used for this fixed parameter as a modelling input
- : Density of the sparged gas (kgm^{-3}). The value of 1.225 was used for this fixed parameter as a modelling input.
- : Density of the liquid in the reactor (kgm^{-3}). The value of 1000 was used for this fixed parameter as a modelling input.
- : Density of the mixture (gas and liquid) in the reactor (kgm^{-3})

References

- Bitog, J.P., Lee, I.-B., Lee, C.-G., Kim, K.-S., et al. (2011) Application of computational fluid dynamics for modeling and designing photobioreactors for microalgae production: A review. *Computers and Electronics in Agriculture*. [Online] 76 (2), 131–147. Available from: doi:10.1016/j.compag.2011.01.015 [Accessed: 28 August 2014].
- Camarasa, E., Carvalho, E., Meleiro, L. a. ., Maciel Filho, R., et al. (2001) Development of a complete model for an air-lift reactor. *Chemical Engineering Science*. [Online] 56 (2), 493–502. Available from: doi:10.1016/S0009-2509(00)00253-0.
- Chisti, Y. (1989) *Airlift Bioreactors*. Elsevier Applied Science Ltd.
- Clift, R., Grace, J. & Weber, M. (1978) *Bubbles, Drops and Particles*. Academic Press.
- Fernandez, F.G., Sevilla, J.M., Perez, J.A., Molina Grima, E., et al. (2001) Airlift-driven external-loop tubular photobioreactors for outdoor production of microalgae : assessment of design and performance. *Chemical Engineering Science*. 562721–2732.
- García-Calvo, E., Rodríguez, A., Prados, A. & Klein, J. (1999) A fluid dynamic model for three-phase airlift reactors. *Chemical Engineering Science*. 542359–2370.
- Gaudin, A.M. (1957) *Flotation*. Second. McGraw-Hill.
- Ishii, M. & Zuber, N. (1979) Drag Coefficient and Relative Velocity in Bubbly, Droplet or Particulate Flows. *American Institute of Chemical Engineers Journal*. 25 (5), 843–855.
- Karamanev, D.G. & Nikolov, L.N. (1992) Free Rising Spheres Do Not Obey Newton's Law for Free Settling. *American Institute of Chemical Engineers Journal*. 38 (11), 1843–1846.
- Kuiper, G. (2010) Physics of cavitation: gas content and nuclei. In: *Cavitation on ship propellers*. Delft, TU Delft. pp. 9–79.
- Kumar, K., Dasgupta, C., Nayak, B., Lindblad, P., et al. (2011) Development of suitable photobioreactors for CO₂ sequestration addressing global warming using green algae and cyanobacteria. *Bioresource Technology*. 1024945–4953.

- Law, D. & Battaglia, F. (2013) Numerical Simulations for Hydrodynamics of Air-Water External Loop Airlift Reactor Flows With Bubble Break-Up and Coalescence Effects. *Journal of Fluids Engineering*. [Online] 135 (8), 081302. Available from: doi:10.1115/1.4024396 [Accessed: 22 October 2014].
- Marquez, M.A., Saez, A.E., Carbonell, R.G. & Robert, G.W. (1999) Coupling of Hydrodynamics and Chemical Reaction in Gas-Lift Reactors. *American Institute of Chemical Engineers Journal*. 45 (2).
- McCabe, W.L., Smith, J.C. & Harriot, P. (1956) *Unit Operations of Chemical Engineering*. 6th edition. Mc Graw Hill International Edition.
- Merchuk, J. (2003) Airlift bioreactors: review of recent advances. *The Canadian Journal of Chemical Engineering*. 81 (June-August), 324–337.
- Merchuk, J. & Siegel, M. (1988) Air-lift reactors in chemical and biological technology. *Journal of Chemical Technology & Biotechnology*. 41105–120.
- Molina, E., Fernández, J., Acién, F. & Chisti, Y. (2001) Tubular photobioreactor design for algal cultures. *Journal of Biotechnology*. 92 (2), 113–131.
- Moo-Young, M. & Chisti, Y. (1994) Bioreactor applications in waste treatment. *Resources, Conservation and Recycling*. 1113–24.
- Morisson, F.A. (2013) *An Introduction to Fluid Mechanics*. New York, Cambridge University Press.
- RH Perry, DW Green, & JO Maloney (eds.) (1999) *Perry's Chemical Engineers' Handbook*. 7th edition. The McGraw-Hill Companies, Inc.
- Petersen, E.E. & Margaritis, A. (2001) Hydrodynamic and Mass Transfer Characteristics of Three-Phase Gaslift Bioreactor Systems. *Critical Reviews in Biotechnology*. 1 (4), 233–294.
- Reckhow, K.H. & Chapra, S.C. (1983) *Data Analysis and Empirical Modeling*. In: *Engineering Approaches for Lake Management*. Butterworth, Boston.
- Sáez, A., Marquez, M., Roberts, G. & Carbonell, R. (1998) Hydrodynamic model for gas-lift reactors. *American Institute of Chemical Engineers Journal*. 44 (6), 1413–1423.
- Shah, Y., Kelkar, B., Godbole, S. & Deckwer, W.-D. (1982) Design parameters estimations for bubble column reactors. *American Institute of Chemical Engineers Journal*. 28 (3), 353–379.
- Softonic International S.L. (2014) ImageJ. [Online]. 2014. Scriptable Java app for scientific image processing. Available from: <http://imagej.en.softonic.com/download>.
- Young, M., Carbonell, R. & Ollis, D. (1991) Airlift bioreactors: analysis of local two-phase hydrodynamics. *American Institute of Chemical Engineers Journal*. 37 (3), 403–428.
- Zhang, T., Wang, J., Wang, T., Lin, J., et al. (2005) Effect of internal on the hydrodynamics in external-loop airlift reactors. *Chemical Engineering and Processing: Process Intensification*. [Online] 44 (1), 81–87. Available from: doi:10.1016/j.cep.2004.05.003 [Accessed: 27 October 2014].
- Zimmerman, W., Zandi, M., Bandulasena, H., Tesař, V., et al. (2011) Design of an airlift loop bioreactor and pilot scales studies with fluidic oscillator induced microbubbles for growth of a microalgae *Dunaliella salina*. *Applied Energy*. 883357–3369.